Cell Host & Microbe
Article

Initial Symbiont Contact Orchestrates Host-Organ-wide Transcriptional Changes that Prime Tissue Colonization

Natacha Kremer,[1,*] Eva E.R. Philipp,[2] Marie-Christine Carpentier,[3] Caitlin A. Brennan,[1] Lars Kraemer,[2] Melissa A. Altura,[1] René Augustin,[1] Robert Häsler,[2] Elizabeth A.C. Heath-Heckman,[1] Suzanne M. Peyer,[1] Julia Schwartzman,[1] Bethany A. Rader,[1] Edward G. Ruby,[1] Philip Rosenstiel,[2] and Margaret J. McFall-Ngai[1,*]
[1]Department of Medical Microbiology and Immunology, University of Wisconsin-Madison, Madison, WI 53706, USA
[2]Cell Biology, Institute of Clinical Molecular Biology, Christian-Albrechts University Kiel, 24105 Kiel, Germany
[3]Laboratoire de Biométrie et Biologie Evolutive, UMR CNRS 5558, Université Lyon 1, Université de Lyon, 69622 Villeurbanne, France
*Correspondence: natacha.kremer@normalesup.org (N.K.), mjmcfallngai@wisc.edu (M.J.M.-N.)
http://dx.doi.org/10.1016/j.chom.2013.07.006

SUMMARY

Upon transit to colonization sites, bacteria often experience critical priming that prepares them for subsequent, specific interactions with the host; however, the underlying mechanisms are poorly described. During initiation of the symbiosis between the bacterium *Vibrio fischeri* and its squid host, which can be observed directly and in real time, approximately five *V. fischeri* cells aggregate along the mucociliary membranes of a superficial epithelium prior to entering host tissues. Here, we show that these few early host-associated symbionts specifically induce robust changes in host gene expression that are critical to subsequent colonization steps. This exquisitely sensitive response to the host's specific symbiotic partner includes the upregulation of a host *endochitinase*, whose activity hydrolyzes polymeric chitin in the mucus into chitobiose, thereby priming the symbiont and also producing a chemoattractant gradient that promotes *V. fischeri* migration into host tissues. Thus, the host responds transcriptionally upon initial symbiont contact, which facilitates subsequent colonization.

INTRODUCTION

Bacterial partners, whether beneficial or pathogenic, often travel great distances from the initial site of contact to their eventual location of sustained colonization within the animal host. For example, the journey of a bacterium through the mammalian digestive tract to its target tissues in the hindgut is equivalent to the host animal migrating hundreds of kilometers. During such a journey, the microbes necessarily pass through a series of chemically and physically distinct environments that, in the case of some pathogens, primes them for colonization of a specific tissue (Krukonis and DiRita, 2003; Alvarez-Ordóñez et al., 2011). For example, exposure and subsequent response to acid stress of the stomach render *Vibrio cholerae* more effective at colonizing the intestine (Merrell et al., 2002); similarly, intracellular passage through a protist in the rumen enhances the pathogenicity of some *Salmonella enterica* strains (Rasmussen et al., 2005; Carlson et al., 2007). However, because symbiotic initiation is difficult to observe under natural conditions and many models bypass the normal inoculation route, questions about in vivo site-specific colonization by a microbial species have remained largely unexplored, such as how does the passage through various host environments affect their ability to colonize a specific site, and what is the molecular nature of the host-symbiont dialog underlying the process?

The acquisition of the bacterial symbiont *Vibrio fischeri* by its squid host *Euprymna scolopes* offers the rare opportunity to probe colonization by specific bacteria directly and in real time in an intact, natural symbiosis using imaging technology. Although the process occurs across a distance of only ~100 μm, it is highly complex. In the established association, in which the symbiont population resides along the apical surfaces of microvillous epithelia within the crypts of the light organ, *V. fischeri* is the exclusive partner; i.e., in its absence, no other bacteria can colonize the organ.

Confocal microscopy has revealed that during passage to this site, *V. fischeri* cells interact first with a pair of juvenile-specific mucociliary epithelial surfaces on the light organ's exterior (Figure 1A), which are concomitantly exposed to thousands of other environmental bacteria. A series of events in the first 3 hr following hatching results in the specific enrichment of the symbiont along these surfaces. At environmentally relevant concentrations of *V. fischeri* (~5,000 cells/ml of seawater), only 3–5 *V. fischeri* cells eventually attach to the cilia (Altura et al., 2013) and aggregate above the pores on the organ's surface (Yip et al., 2006). Once aggregated, this population migrates to and through the pores, and then down the ducts to a physical bottleneck where one or two bacteria squeeze into each crypt and proliferate, filling the spaces. Only *V. fischeri* can negotiate this journey beyond the pores (McFall-Ngai and Ruby, 1991).

Studies of the system indicate that the chemistry of the mucus is an important determinant of the events leading to colonization. During aggregation, other bacterial species are excluded as *V. fischeri* cells become primed for their colonization process. In brief, within seconds of hatching from the egg, the animal begins ventilating seawater through its body cavity and shedding mucus from the epithelial surface of the nascent light organ as a nonspecific response to cell-wall (peptidoglycan) derivatives

A

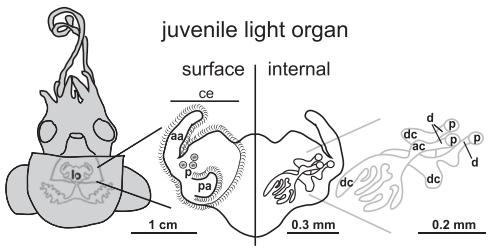

B

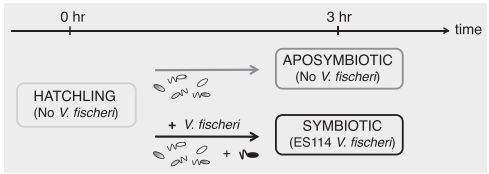

C

454 sequencing (raw data)		
	Number of sequenced bases	499,197,328
	Number of reads	2,087,030
	Median length before assembly (bp)	305
Assembly (Newbler v2.6)		
	Number of reads assembled	1,645,954
	Mean transcriptome size (bp)	20,756,385
	Number of isogroups	21,966
	Number of isotigs	27,031
Features of assembled sequences		
	% GC	36.2
	% annotation	47.3
	Median length after assembly (bp)	700

D

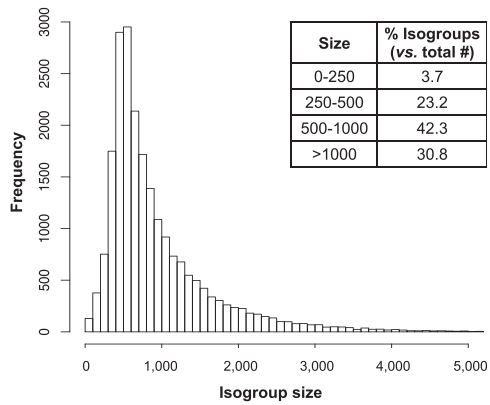

Size	% Isogroups (*vs.* total #)
0-250	3.7
250-500	23.2
500-1000	42.3
>1000	30.8

E

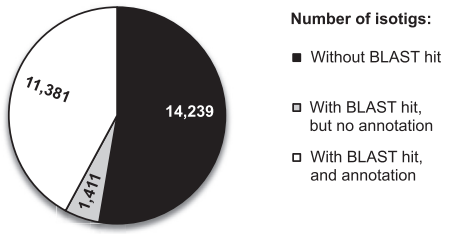

Figure 1. Symbiotic Organ Structure, Experimental Setup, and Generation of the Squid Light-Organ Transcriptome

(A) Left: Diagram of the ventral surface showing the light organ (lo) suspended in the body cavity, visible in this drawing through the translucent mantle. Center: Enlargement of the light organ showing the surface in contact with the seawater (left) and the internal structure through which symbionts migrate (right). Right: Detailed anatomy of the three crypts. ce, ciliated epithelium; p, pore; aa, anterior appendage; pa, posterior appendage; dc, deep crypt; ac, antechamber; d, duct.

(B) Experimental setup for the collection of squid used for 454 sequencing. Squid were incubated for 3 hr in seawater containing ~10^6 environmental bacteria ± 5,000 *V. fischeri* cells/ml.

(C) General statistics on 454 sequencing and assembly.

(D) Size distribution of isogroups after assembly.

(E) Summary of the GO annotation results, using the score function of the Blast2GO software. This process consists of a BLAST annotation against databases and a mapping step for the assignation of GO terms.

See also Figure S1.

released by environmental bacteria (Nyholm et al., 2002). The mucus matrix contains antimicrobial biomolecules (Troll et al., 2010) and vesicles containing nitric oxide (NO) (Davidson et al., 2004). As in other host-symbiont interactions, including the highly complex mammalian-microbiota alliances (Duerkop et al., 2009), these antimicrobials provisioned into the mucus may create a selective "cocktail" that functions in specificity and stability of the associations.

V. fischeri responds to this specific environment presented by the host during aggregation; e.g., the low concentration of NO present in the mucus upregulates NO-detoxification mechanisms (Wang et al., 2010), which protect the symbiont against the more acute NO stress subsequently encountered in the ducts. Additionally, chemotaxis by *V. fischeri* mediates migration into the host tissues in response to signals like the dimeric breakdown product of chitin, chitobiose (di-*N*-acetyl-glucosamine) (Mandel et al., 2012). Thus, bacterial symbionts respond both transcriptionally and behaviorally to the host-derived conditions they encounter during initiation.

Here we show that, although exposed to the myriad of other bacteria in the seawater, host tissues respond to the few attaching *V. fischeri* cells with significant changes in gene expression, most notably in genes encoding proteins that alter the environment to favor symbiont colonization. To explore the impact of symbiont-induced host transcription on the environment presented to the symbiont, we examined in depth one upregulated gene and its encoded protein, a chitotriosidase. We provide evidence that symbiont-induced upregulation of the host *chitotriosidase* gene results in two downstream events: a priming of *V. fischeri* by shaping of the biochemistry, wherein they aggregate before entering host tissues, an activity that primes the symbiont for responses to chitin polymers; and the production of a gradient of chitobiose that mediates effective symbiont migration into host tissues. These studies provide a detailed window into the first minutes to hours of interaction between the tissues of a host animal and its symbiotic partner.

RESULTS

The Transcriptome of the Nascent Organ Is Diverse

To determine whether changes in gene expression accompany early symbiotic events, we first constructed a reference

transcriptome (Figure 1). Libraries built from extracted organs included (1) "hatchling," <15 min after hatching from the egg; (2) "aposymbiotic," 3 hr after hatching and incubation in Hawaiian offshore seawater (HOSW), which contains environmental bacteria (~10^6/ml) but is devoid of *V. fischeri*; and (3) "symbiotic," the "aposymbiotic" condition, but with wild-type *V. fischeri* added at a typical, field-relevant concentration of ~5,000 cells/ml (Figure 1B).

This database of early-stage symbiosis increased the number of known transcripts for the *E. scolopes* light-organ transcriptome by ~40% over a previously constructed Expressed Sequence Tags database (Chun et al., 2006). Pyrosequencing yielded about 2 × 10^6 reads, from which 79% were assembled, with an inferred read error of 1.5%–2.4% (Figure 1C; Figure S1C available online). Assembly yielded >20,000 isogroups, i.e., unique sequence assemblies potentially representing gene loci, with a median length of 700 bp (Figures 1C and 1D) and mean coverage of 12×. These isogroups were constituted on average by 1.23 isotigs, alternative transcripts associated with a single locus. About 47% of the isotigs could be annotated by Blast2GO software (Figure 1E) with relatively high similarity and low e-values (Figures S1D and S1E). These annotations were inferred principally from UniProt Knowledgebase by electronic annotation against several animal species (Figures S1F–S1H). Each annotated isotig was assigned an average of 4.8 Gene Ontology (GO) terms (Figures 1E and S1I–S1K). Assignment to Cluster of Orthologous Groups revealed enrichment of clusters related to cellular processes and signaling (39%) compared with information storage and processing (21%) and metabolism (19%); 21% were poorly characterized (Figure S1L).

Only a Few *V. fischeri* Cells Are Needed for Inducing Specific Changes in Host Gene Expression

We compared the transcriptome of symbiotic organs during the aggregation of the group of approximately five *V. fischeri* cells with that of aposymbiotic organs. It is important to note that these aggregating *V. fischeri* cells were in contact with only two to three host cells, although the libraries were generated with entire juvenile organs, which have approximately 10^4 eukaryotic cells each. As such, any changes in the inductive signal from *V. fischeri* must be either highly upregulated in the two to three interacting host cells or spread across the entire organ. Recent studies also indicate that, at low bacterial inoculum, *V. fischeri* products that probably induce host responses would be in concentrations too low to cause these widespread effects (Altura et al., 2013).

We first analyzed a subset of the 3 hr symbiotic animals, obtained concurrently with tissue harvested for the production of the reference transcriptome, to confirm that an average of 5.2 ± 0.8 *V. fischeri* cells directly interact with squid tissues after a 3 hr incubation (Altura et al., 2013; Figures 2A, S1A, and S1B). Examination of the 454-sequencing libraries identified 84 isotigs (0.31% of the total) differentially represented between the aposymbiotic and symbiotic conditions, of which 72% had annotations (Figure 2B; Table S1). Functional enrichment analysis of these differentially expressed isotigs revealed two major predicted molecular signatures of first contact between symbiotic partners: protease and hydrolase activities directed at sugar bonds, especially those associated with chitin metabolism (Figure 2C). None of these transcripts were differentially regulated in the hatching compared to the aposymbiotic condition (Table S1). Taken together, the data demonstrate that the changes in the transcription of the 3 hr symbiotic light organ are due to host-tissue discrimination of only a few associating *V. fischeri* cells.

To reveal changes in gene expression that would result from exposure to nonspecific environmental microbes and/or post-embryonic development over the first 3 hr posthatch, we also compared the transcriptomes of hatchling light organs to those of the aposymbiotic condition. Based on functional enrichment analysis, we detected a significant differential representation of transcripts only in GO terms associated with the ribosomal machinery (Table S1). This differential expression is also detectable between hatchling and symbiotic light organs (Table S1).

Focusing on molecular signatures highlighted by functional analysis in the symbiotic condition, we confirmed the RNA sequencing (RNA-seq) results by determining expression of isotigs encoding proteins associated with protease activity (chymotrypsin protease, cathepsin L, and legumain) and chitin metabolism (chitotriosidase) by quantitative RT-PCR (qRT-PCR) (Figures 2D and 2E). Additionally, we tested differentially expressed isotigs encoding proteins involved in immune responses to bacteria (ferritin and lysozyme). We assayed squid light organs from multiple egg clutches (seven individual clutches laid by different captive females, thus with different genetic backgrounds) to control for genetic variability that may influence development and responsiveness to a symbiotic infection. Five of the seven clutches responded to contact with *V. fischeri* by upregulating a set of several isotigs encoding, in order of highest to lowest fold change, chymotrypsin protease, lipase, chitotriosidase, legumain, cathepsin L, lysozyme, and ferritin. The overall within-clutch patterns were consistent; i.e., all of these genes were either upregulated or not regulated in the organs of a given clutch. Despite this biological variability, these data demonstrate that the ciliated epithelial cells are able to sense the few associating *V. fischeri* cells, in a background of 10^6 nonsymbiotic bacterial cells, and induce specific transcriptional changes in the juvenile light organ.

A Catalytically Active Chitotriosidase Localizes to the Apical Surfaces of Epithelial Cells, Pores, and Ducts of the Organ Surface and Is Secreted into the Associated Acidic Mucus Matrix

Because chitin and its breakdown products play major roles in both the establishment and maintenance of the symbiosis (Wier et al., 2010; Heath-Heckman and McFall-Ngai, 2011; Miyashiro et al., 2011; Mandel et al., 2012), as well as in the pathogenesis of other *Vibrio* species (Meibom et al., 2005; Blokesch and Schoolnik, 2007), we chose to focus on an in-depth characterization of the symbiont-induced *chitotriosidase* gene and its encoded protein.

Analysis of the derived amino-acid sequence of this putative chitotriosidase supported its role in chitin degradation. Based on the full-length sequence of *EsChitotriosidase* obtained by rapid amplification of complementary DNA (cDNA) ends (RACE), the encoded protein was similar in sequence (Figure S2) and tertiary structure (Figure 3A) to a highly conserved animal endochitinase. Chitotriosidase catalyzes the random hydrolytic cleavage of β-1,4 glycosidic bonds of the chitin polymer; as an

A

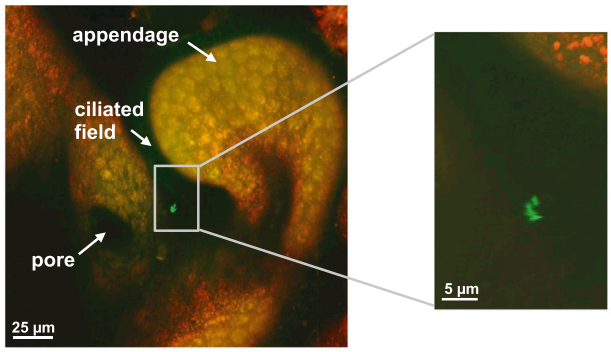

B

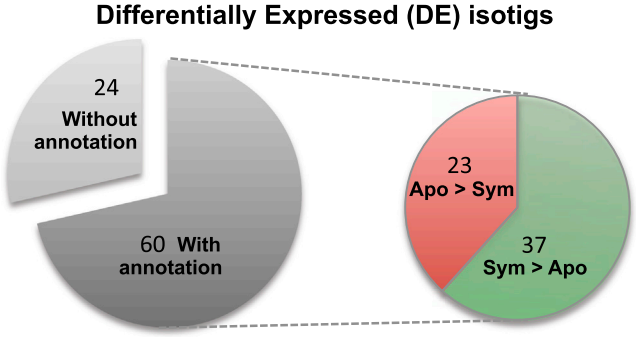

C

Molecular functions differentially represented

GO Level	GO term number	ratio (log)	adj. p value	GO term description
MF3	0016787	1.50	5.05E-3	Hydrolase activity
MF4	0008233	2.41	8.43E-4	Peptidase activity
	0016798	3.43	3.76E-2	Hydrolase activity (glycosyl bonds)
MF5	0070011	2.23	4.32E-2	Peptidase activity (L-amino acid peptides)
	0004553	3.61	4.32E-2	Hydrolase activity (O-glycosyl compounds)

D

Isotigs differentially expressed by qRT-PCR

Gene name used in the study	RNAseq in silico analysis		qRT-PCR Symbiotic/ Aposymbiotic ratio	
	R_j statistics	Reliability	fold change	p value
Lipase	39.60	*	4.48	*
Ferritin	21.84	*	2.90	*
Chymotrypsin protease	12.63	*	5.21	*
Cathepsin L	7.65	*	4.12	*
Chitotriosidase	7.20	*	4.34	*
Legumain	2.92	·	4.28	*
Lysozyme	2.07	·	3.95	*

E

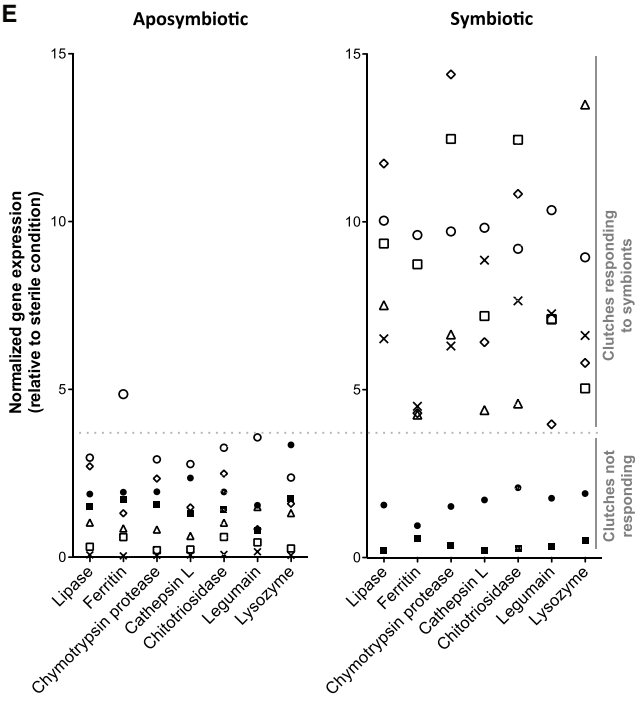

Figure 2. Effect of Contact with *V. fischeri* on the Expression of Host Genes

(A) Confocal images showing an aggregate of four *V. fischeri* cells (GFP-ES114, green) in association with host tissues (CellTracker Orange).

(B) Distribution of the differentially expressed isotigs between aposymbiotic (Apo) and symbiotic (Sym) light-organ libraries.

(C) Functional enrichment analysis based on molecular functions (MF) (FatiGO software). Ratios correspond to the percentage of a particular GO term in the list containing differentially expressed isotigs divided by its percentage in the reference list (aposymbiotic condition). MFs 1, 2, 6, 7, 8, and 9 did not exhibit any significant GO terms.

(D) Summary of differential expression of candidate genes based on in silico database analysis (R_j statistics from Stekel et al., 2000; *, $R_j > 3$;., $R_j > 2$) and qRT-PCR (n = 7 clutches, data detailed in E; *$p < 0.05$ with paired t test between aposymbiotic and symbiotic conditions followed by false discovery rate adjustment).

(E) Differential expression of candidate genes by qRT-PCR (n = 7 clutches from different females, each represented by a different symbol). Expression of candidate genes was first normalized to the expression of three housekeeping genes. The expression data from aposymbiotic and symbiotic light organs, originating from squid incubated for 3 hr in HOSW, were then normalized to the expression data from aposymbiotic light organs originating from squid incubated for 3 hr in FSIO (the sterile condition).

See also Table S1.

endochitinase, it releases chitobiose and larger multimers, but not the monomer, GlcNAc. It contains a signal peptide for secretion, a glycosyl hydrolase 18 (GH18)-type catalytic domain with the critical DxxDxDxE residues essential for activity (Fusetti et al., 2002) (SWISS-MODEL *Z* score = −2.53 against human chitotriosidase complexed with chitobiose; Benkert et al., 2011) and two chitin-binding domains with conserved cysteine residues critical for substrate binding. As such, it is predicted to be a secreted, catalytically active protein. We confirmed its catalytic activity using affinity-purified EsChitotriosidase (Figures 3B and 3C).

With microscopy, we localized the encoding transcript and the protein in the light organ. Whole-mount in situ hybridization (ISH) revealed abundant transcript in the superficial ciliated epithelium and the cells surrounding the light-organ pores (Figure 3D). Confocal immunocytochemistry localized the protein

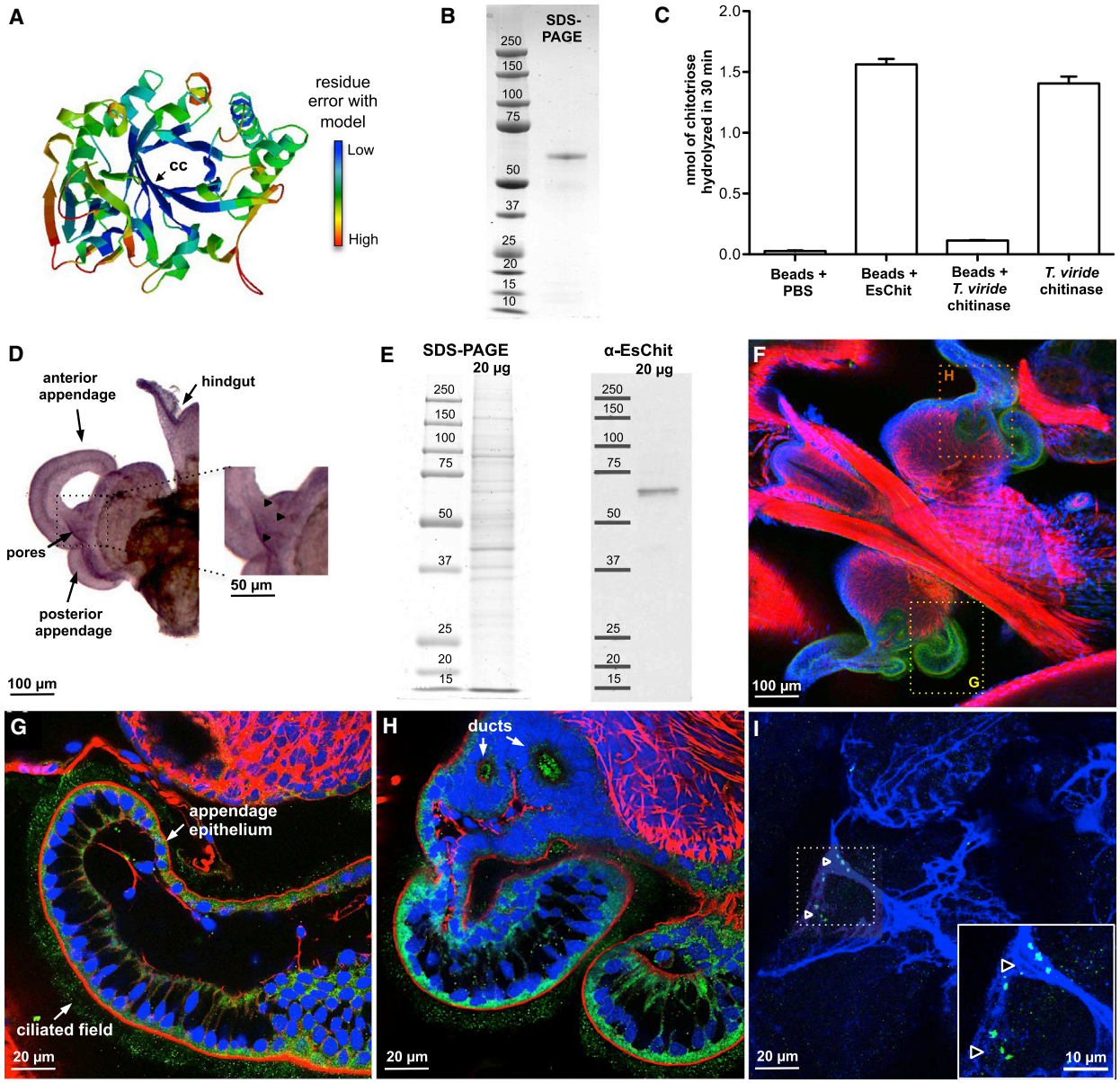

Figure 3. Localization of Chitotriosidase in the Squid Light Organ and Protein Characterization

(A) Predicted three-dimensional structure of the catalytic chitotriosidase (EsChit) GH18 domain. Swiss-Prot model: crystal structure of human chitotriosidase in complex with chitobiose (1LG1; Fusetti et al., 2002). Although the protein sequences are only 46% identical, the structure of EsChit is predicted to be similar to that of human chitotriosidase (Z score = −2.53), especially in the proximity of the chitobiose-binding site (cc, catalytic center). The gradient from cold to warm colors corresponds to residue error compared to the human chitotriosidase structure.

(B) SDS-PAGE gel of purified EsChit (SYPRO Ruby staining).

(C) Chitotriosidase activity of EsChit purified using chitin-magnetic beads (mean ± SE; measurements done in triplicate). The activity was measured in assay buffer (Sigma). Chitinase (100 ng) from the fungus *Trichoderma viride* (*T. viride*; Sigma) was used as a positive control for the effect of binding to beads on chitinase activity.

(D) ISH of *EsChit* in a symbiotic light organ (antisense probe). Purple staining, corresponding to the RNA expression of *EsChit*, is particularly high in the proximity of the pores (triangles, inset), in the epithelium of the appendages, and in the hindgut.

(E) Coomassie staining of an SDS-PAGE gel of squid-tissue soluble-protein extract (left) and its associated western blot against EsChit (right, expected size: 59.2 kDa without signal peptide).

(F–I) ICC of EsChit in the light organ (F). The antigen labeling is particularly bright in the ciliated field and the cytosol of the appendage epithelium (G) and in the pores and ducts region (H). Colored boxes in (F) show representative locations of pictures zoomed in panels (G) and (H). Green, α-EsChit; red, rhodamine phalloidin (f-actin); blue, TOTO-3 (nuclei). (I) ICC of EsChit in the mucus coating the appendage epithelium. Triangles indicate foci of the protein in the mucus. The inset is a higher magnification of the region highlighted by the box. Green, α-EsChit; blue, Alexa 633 WGA (mucus-binding lectin WGA). Negative controls for ISH (sense probe) and ICC, as well as the RACE sequence of *EsChit* and its predicted domains and functional residues, are presented in Figure S2.

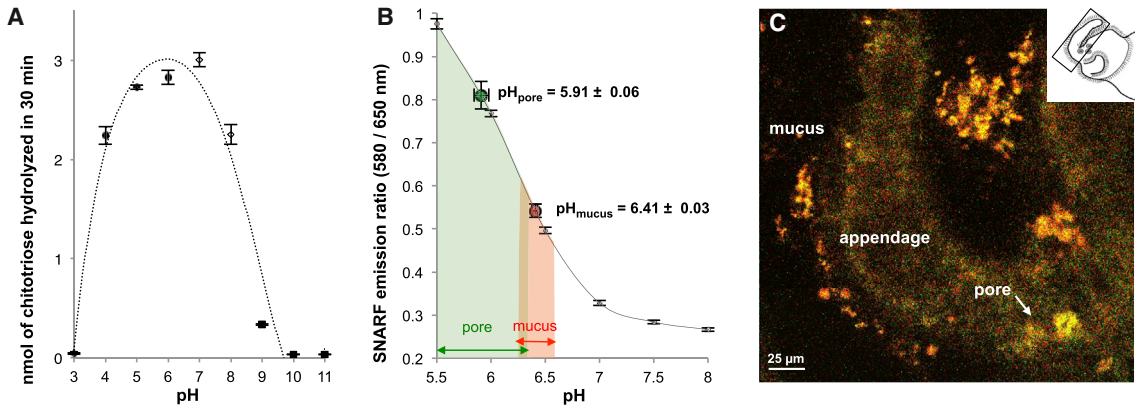

Figure 4. The Activity of EsChitotriosidase in Relation to the pH Measured at the Light-Organ Surface

(A) Effect of pH on EsChitotriosidase activity (mean ± SE; measurements done in triplicate; black dotted line, polynomial regression). Activity in 2.5% NaCl was measured: (◆), at pH 3, 4, 5, and 6 in 100 mM sodium acetate; (◇), at pH 7 and 8 in 100 mM Tris; (■), at pH 9, 10, and 11 in 100 mM sodium carbonate.

(B and C) pH was estimated using WGA coupled to a pH-sensitive fluorescent probe (SNARF). This probe is excited at 488 nm and selectively emits at two different wavelengths (580 nm and 650 nm). The emission ratio is characteristic of a specific pH, estimated by a calibration curve. (B) Determination of pH; mean ± SE; n = 10 squid (ten measurements per squid). The red and green areas indicate the range of pH values observed in the mucus and around the pores, respectively. The calibration curve (gray) was generated in pH-adjusted mPBS; mean ± SE; n = 20 measurements. (C) Example of WGA-SNARF staining in the mucus coating the appendage and in the pore. Gradient colors from yellow-red (in the mucus) to green-yellow (close to the pore) match with a mild-acidic to an acidic pH, respectively. The inset orientates the imaged tissue within the light organ.

to intracellular regions along the apical surfaces of the cells of the ciliated field, pores and ducts of the organ (Figures 3E–3H). In addition, the antibody recognized the secreted protein in the mucus matrix overlying the light-organ ciliated surface (Figure 3I). These data demonstrate that the gene is transcribed and the protein produced and secreted in locations where *V. fischeri* aggregates and establishes dominance over other seawater bacteria.

The EsChitotriosidase Occurs in Sites with an Optimal pH for Its Activity

Using a chitinase activity assay, we determined that the pH optimum for in vitro endochitinase activity (i.e., the conversion of chitotriose to chitobiose) of the EsChitotriosidase is between pH 5.0 and 7.5 (Figure 4A), typical of chitotriosidases (e.g., Xu and Zhang, 2012). Because the pH of the seawater surrounding the squid in nature (~8.2) is well above this range, we hypothesized that the environment created by the host in the location where *V. fischeri* aggregates is more acidic. To determine the pH of the ciliary-mucus environment, we constructed a pH-sensitive probe coupled to wheat-germ agglutinin (WGA), a lectin known to bind the mucus (Nyholm et al., 2002). The pH in the mucus along the organ's ciliated appendages was approximately 6.4, and it was 5.9 in the region of the pores (Figures 4B and 4C). Thus, the mucus matrix has a pH range different from that of the seawater passing over these tissues but compatible with the optimal pH for EsChitotriosidase activity. No difference in pH was observed in these regions over the first 3 hr following hatching under any condition; i.e., interaction of host tissues with *V. fischeri* cells did not influence the pH.

Chitin Derivatives Are Presented in the Mucus and Ducts where the EsChitotriosidase Occurs

To present *V. fischeri* with chitobiose for either priming or the creation of a chemoattractant gradient, the host chitotriosidase must have the substrate chitin, the production of which has been shown to be dependent on chitin synthase in other systems. A chitin synthase localized mainly to the apical surfaces of the ciliated epithelia and to regions of the pores and ducts (Figure 5A). For chitin, we used three different labeling methods. A previous study with a chitin-binding protein (CBP; New England Biolabs) that detects polymers larger than hexamers showed no labeling at the pores or in the ducts (Heath-Heckman and McFall-Ngai, 2011); this study did not examine the mucus. Using a fix to preserve the mucus, the CBP labeled chitin polymers in the mucus matrix (Figure 5B). In animal tissues, calcofluor white binds to polysaccharides. This reagent labeled strongly in regions of the pores and ducts (Figure 5C). To characterize the type of polysaccharides present in these regions, we performed a complementary staining method capable of differentiating GlcNAc and small chitin breakdown products from sialic acid. GlcNAc residues were present on the organ surface and to ~10–12 µm into the ducts; in contrast, only sialic acid residues were present farther down in the ducts (Figures 5G–5I). These results suggest a relative enrichment of small polymers of chitin surrounding the pore and superficial duct regions, where *V. fischeri* senses a chitobiose gradient.

Degradation of Chitin Promotes *V. fischeri* Chemoattraction and Efficient Host Colonization

Although *V. fischeri* cells exhibit chemotaxis toward chitobiose during early symbiotic initiation, laboratory studies directly assaying this behavior suggest that, when grown under the conditions used for squid colonization experiments, these bacteria exhibit minimal chemotaxis toward chitobiose (Figure S3). Given that EsChitotriosidase is localized not only close to the pores, but also in the mucus along the ciliated field (Figure 3I), we hypothesized that (1) the EsChitotriosidase activity would produce low levels of chitin breakdown products in the mucosal environment; and (2) during aggregation, *V. fischeri* cells would be

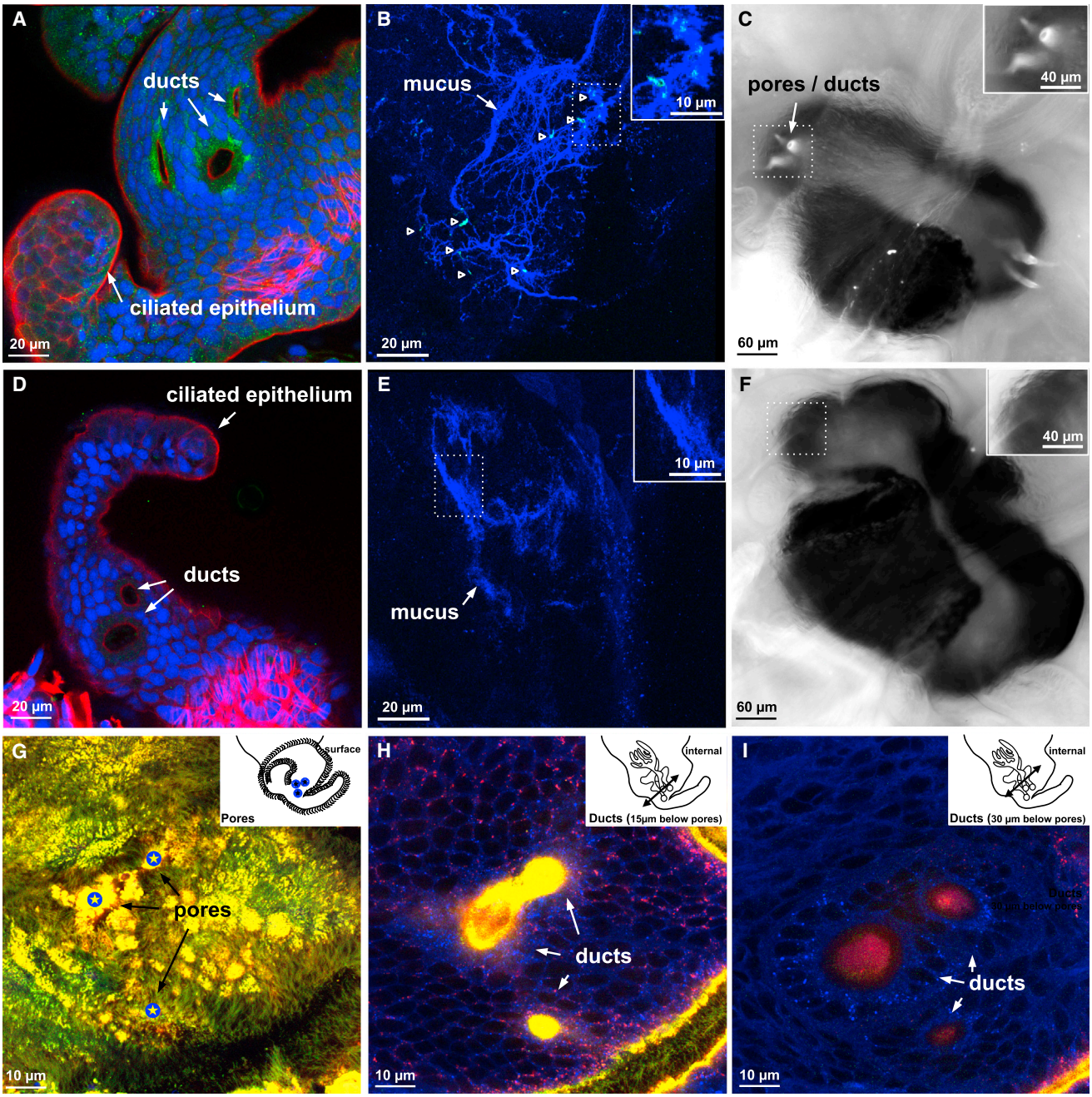

Figure 5. Expression of Chitin Synthase and Presence of Chitin Derivatives in the Squid Light Organ

(A and D) Immunocytochemical localization of *E. scolopes* chitin synthase (EsCS). (A) Expression of EsCS in duct cells. (D) The negative control using IgY instead of the antibody, because the EsCS antibody was generated in chicken. Green, α-EsCS (A) or α-IgY (D); red, rhodamine phalloidin (f-actin); blue, TOTO-3 (nuclei).

(B and E) Localization of chitin in the mucus surrounding the ciliated appendages. (B) Chitin residues in the mucus labeled with CBP. (E) Negative control, without added CBP. Inset: Magnification of the boxed region. Green, FITC-CBP (chitin); blue, WGA (mucus).

(C and F) Localization of polysaccharides in the light organ. (C) Calcofluor staining in the pores and ducts. (F) Negative control, no calcofluor added. Insets: Higher magnification of the pores and ducts region.

(G–I) Confocal images of WGA labeling at different levels, from the pores (blue star) to the ducts. Inset: Illustration showing the location of the section (arrow) along the light organ. Red, Alexa 633 WGA (GlcNAc and sialic-acid residues); green, FITC-succinylated WGA (GlcNAc residues only); blue, CellTracker Orange (animal cells).

presented with these products, priming these cells to subsequently sense the chitin-based chemoattractant gradient that mediates migration into the host ducts. To test whether pre-exposure to chitin breakdown products does in fact increase chemotactic recognition of chitobiose by *V. fischeri*, we preincubated cells in culture medium either with or without added

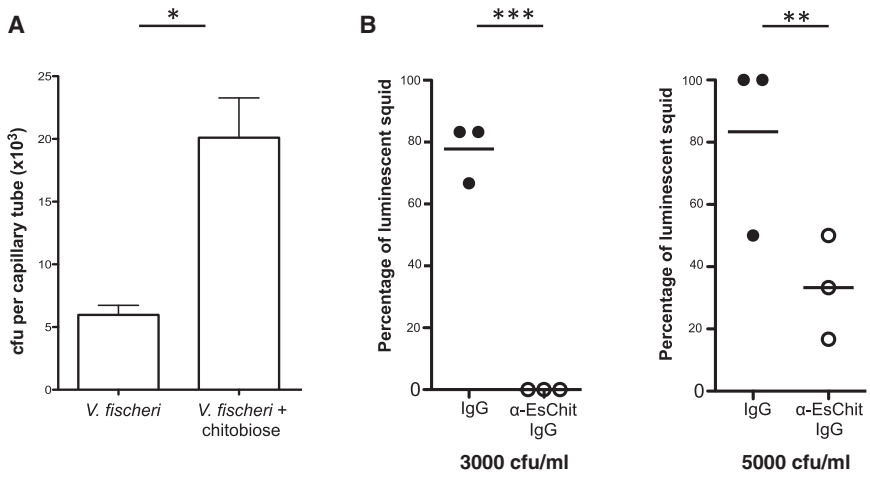

Figure 6. Role of EsChitotriosidase in Early Colonization Events

(A) Importance of priming of *V. fischeri* for chemotaxis toward 10 mM chitobiose, tested using capillary assays (mean ± SE; three biological replicates with two technical replicates each). Pretreatment was performed with 1 mM chitobiose in SWT. Wilcoxon signed-rank test; *$p < 0.05$. See also Figure S3.

(B) Effect of coincubation with α-EsChit antibody on colonization of the light organ by *V. fischeri* using different inocula (n = 3 replicates of six squid per inoculation per condition). Fisher's exact test; ***$p < 0.001$; **$p < 0.01$. The luminescence values reflect differences in cfu colonization levels.

chitobiose and measured their subsequent chemoattraction toward chitobiose using capillary assays (Figure 6A). *V. fischeri* cells that were previously exposed to chitobiose showed increased migration toward chitobiose. These data suggest that exposure of *V. fischeri* to chitin in the aggregate primes the symbionts to later respond to a chitobiose gradient during transit through the pores.

To determine whether EsChitotriosidase played a role in chitobiose priming for symbiont chemotaxis, we measured the effect of the chitotriosidase inhibition on colonization efficiency by adding the α-chitotriosidase antibody (20 μg/ml) to the surrounding seawater as symbionts were initiating colonization. Antibody binding significantly decreased chitotriosidase activity in vitro (ANOVA, treatment: $F = 21.7$, $p = 0.007$; replicate: $F = 18.4$, $p = 0.009$; comparison between anti-EsChitotriosidase (α-EsChit) immunoglobulin G (IgG) and control IgG: $p_{adj} = 0.01$). In vivo efficiency of symbiosis initiation, as measured by the proportion of *V. fischeri*-exposed animals that had been successfully colonized one day after inoculation, was statistically lower in animals that had been exposed to the antibody during initiation (Figure 6B), suggesting that antibody binding of the EsChitotriosidase compromises the ability of the symbiont to colonize normally.

DISCUSSION

In this study, we demonstrate that, during the initiation phase of an animal-bacterial association, partner interactions create an environment that facilitates the species-specific colonization of distant host tissues. In the squid-vibrio symbiosis, the initiation of colonization occurs as a progression of events that cover a distance of only a few tens of microns during the first ~3 hr after the host hatches from its egg. These discrete events have allowed a fine-scale spatiotemporal resolution of the colonization process, leading to the construction of a model describing the host's progression from a state of readiness to one of selective responsiveness (Figure 7). This model illustrates two major findings of our study: (1) the remarkable sensitivity of host gene expression to the presence of just three to five cells of the specific symbiont, and (2) the link between these changes in expression and the symbionts' successful migration into distant tissues.

Much as in the newborn mammal, the juvenile squid hatches from an essentially sterile environment that surrounds the embryo; however, its first postembryonic ventilations bring myriad environmental microbes into the juvenile's body cavity. Perhaps one of the most remarkable observations in the present study is that as few as three to five *V. fischeri* cells are sufficient to induce a specific transcriptional expression pattern in light-organ tissues, suggesting that the animal hatches from the egg in a state of readiness, but is highly selective in its response (Figure 7A). In an analogous manner, although transcriptomic studies of the initial hours of host-microbe interaction have not been conducted in mammals, normal embryonic development and communication across the placenta result in the production of specific cells (e.g., RORγt$^+$ cells; Eberl, 2012) and biomolecules (e.g., maternal antibodies; Blümer et al., 2007) that ready the host's immune system for subsequent early postembryonic exposure to microbes.

The mucociliary membranes of the nascent light organ, where the first steps of colonization occur, have a structure, activity, and biochemistry similar to those of epithelial surfaces of the airway, excretory, and reproductive systems of mammals, as well as of the peritrophic membranes that line the midgut of insects (Dinglasan et al., 2009; Hegedus et al., 2009). For example, in both the squid (Davidson et al., 2004; Troll et al., 2010) and mammalian (Duerkop et al., 2009) model systems, antimicrobial compounds incorporated into the mucus influence the composition of the native microbiota, as well as the successful colonization by potential pathogens. Such symbiont-partner selection has also been explored at the cellular and molecular levels in basal metazoans. Specifically, in certain cnidarian species, the secretion of mucus containing antimicrobial peptides along the apical surfaces of the superficial epithelia is critical for the establishment of the normal community composition of the native microbiota (Fraune et al., 2010). Our data suggest that the mucus matrix of the host squid changes as the nascent tissues modulate their gene expression in response to interactions with *V. fischeri*. It is tempting to speculate that the regulation of squid genes, such as those encoding potentially antimicrobial acidic proteases, iron-sequestering proteins, and chitinases, which all have homologs associated with general inflammatory responses (Cho et al., 2002; Conus and Simon, 2010; Lee et al., 2011), is a

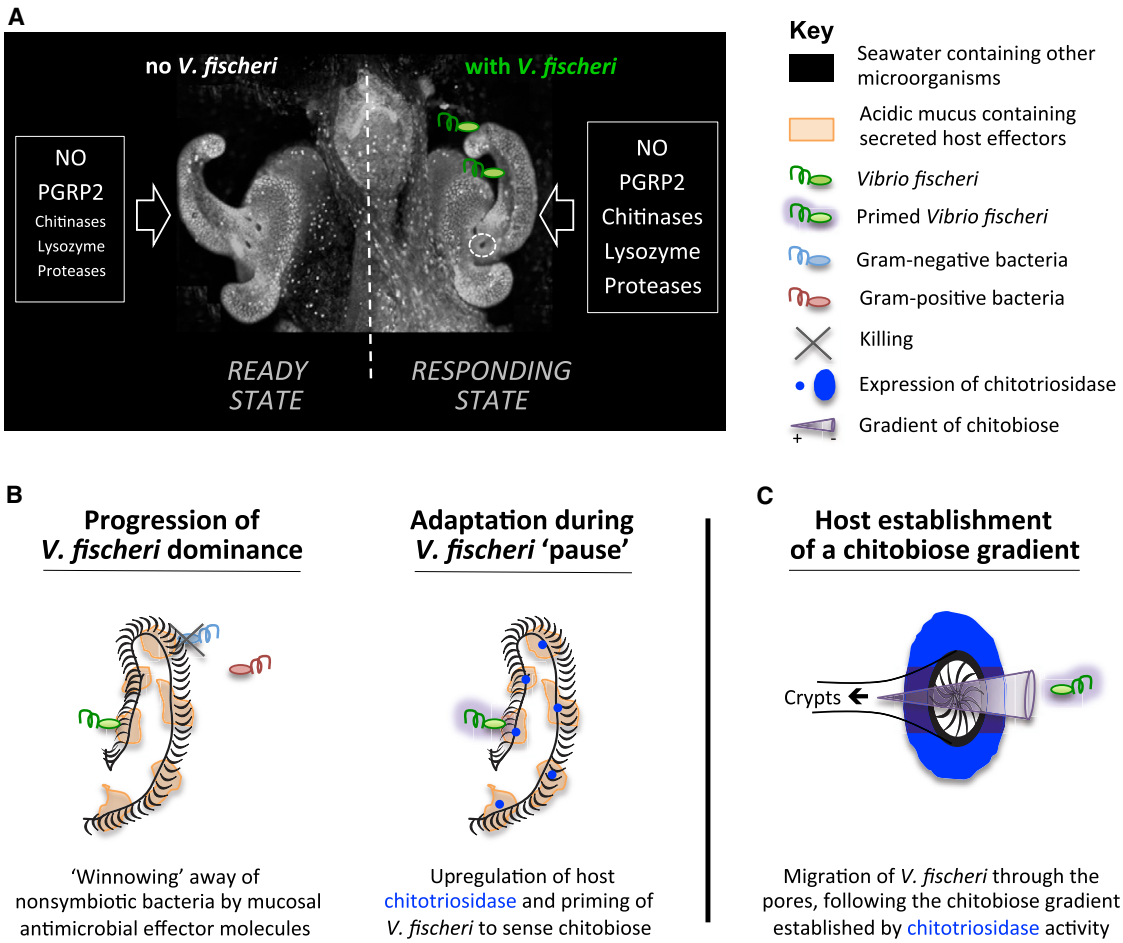

Figure 7. Model for Early Colonization

(A) The initial contact of *V. fischeri* with host tissues induces the expression of several genes (e.g., *proteases*, *chitinases* such as *EsChitotriosidase*, and *lysozyme*) whose products, when supplemented with components already present in the mucus (NO and EsPGRP2), affect the chemistry of the mucus matrix, shaping the specificity and preparing for future colonization events.

(B) Course of events that allow selective colonization by *V. fischeri*. Left: Antimicrobial compounds (e.g., lysozyme and PGRP2) are activated by acidic proteases in the low-pH environment and participate in the selective exclusion of nonsymbiotic bacteria. Right: While *V. fischeri* cells are "pausing" in the aggregate, the upregulation of EsChitotriosidase in the ciliated field of the light organ hydrolyzes chitin into chitobiose, which prepares *V. fischeri* to sense and be attracted toward chitobiose.

(C) EsChitotriosidase, which is highly expressed close to the pores and optimally active at low pH, degrades chitin produced by the host into chitobiose, thereby establishing a chitobiose gradient extending out of the pores. Primed *V. fischeri* cells are attracted by the chitobiose gradient and migrate through the pores (Mandel et al., 2012).

mechanism through which proper symbionts are selected. Interestingly, many of these proteins are regulated in response to microbe-associated molecular patterns in other systems (Ong et al., 2005; Badariotti et al., 2007; Liu et al., 2009) and have activities with optima at a low pH, like that found in the light-organ mucus (Figure 4). Thus, it can be postulated that the matrix on the surface of epithelia is responsible for a type of "ecosystems management," wherein fluid dynamics (e.g., ciliary activity and peristalsis) function together with the biochemistry of the mucus to control microbial associations.

In what ways might such changes in host gene expression also control symbiont specificity and colonization efficiency? In this study, we considered in depth one such *V. fischeri*-induced host gene, encoding EsChitotriosidase, and tested the hypothesis that its degradation of chitin to chitobiose might increase the efficiency of symbiont colonization. Between aggregation and migration, *V. fischeri* cells "pause," a behavior that has been associated with preparation for the upcoming oxidative environment of the duct (Wang et al., 2010) and that may also similarly prime them for other conditions, such as a host-derived chemotactic gradient. Many species of the Vibrionaceae, including *V. fischeri*, are chemotactic toward chitooligosaccharides (Bassler et al., 1991; Hirano et al., 2011), and chitobiose specifically induces a subset of *V. fischeri* genes, including several encoding certain chemotaxis proteins (A. Schaefer, personal communication). In addition, a recent study (Mandel et al., 2012) showed that *V. fischeri* uses chemotaxis toward chitobiose to navigate into host tissues; however, when and how this chemoattractant gradient is produced was not addressed. We showed that the initial host-symbiont contact results in an

upregulation of *EsChitotriosidase*, encoding a protein whose catalytic function releases chitobiose. The data suggest that this activity establishes a chitobiose gradient in the vicinity of the pores and primes the symbionts to induce chitin-responsive gene transcription in the aggregates. As a result, pre-exposure to chitin breakdown products enhances the ability of symbiotic *V. fischeri* cells to subsequently sense a chemoattractant gradient toward chitobiose (Figure 6). Taken together, these results suggest that symbiont induction of host *EsChitotriosidase* shapes the local chemical environment in a way that favors the eventual migration of the symbionts through the pores, and thus efficient establishment of a symbiotic colonization. Chitobiose may not be the only chemoattractant in the system; other chemoattractants may be responsible for bringing the bacteria to their final residence, the crypt spaces. This priming behavior is not unlike that of the human symbiont *Bacteroides thetaiotaomicron*, which responds to host-derived fucose residues by inducing enterocyte glycosylation (Bry et al., 1996). Interestingly, a pathogenic *Escherichia coli* strain has recently been shown to also sense *Bacteroides*-released fucose and, as a result, use it as a cue to induce expression of virulence genes (Pacheco et al., 2012). Whether other hosts produce (oligo)saccharide signals that are used by bacteria to establish a persistent association remains to be determined, but the existing examples already point to the role of such signaling in interdomain communication between coevolved partners (Oldroyd, 2013; McFall-Ngai et al., 2013).

Surprisingly, our results suggest the possibility that interaction with only a few symbiont cells results in the propagation of a transcriptional signal for *EsChitotriosidase* across the ~10,000 cells of the entire organ; i.e., the pattern revealed by ISH provides evidence that the induction of gene expression is not confined to the few host cells directly interacting with the symbiont aggregate (Figure 2A), but is shared by much of the ciliated surface epithelium. These results contrast with a previous study of whole light organs in which ISH indicated that a symbiont-induced increase in expression of the C8 subunit of the proteasome was confined to one cell type in the ciliated fields (Kimbell et al., 2006). The results of the present study suggest that localized signaling by *V. fischeri* cells not only promotes specificity on the ciliated surface and migration into host tissues, but also may prepare distant tissues (e.g., the crypt epithelium) for eventual colonization by the symbiont. More refined techniques, such as laser-capture microdissection (Hooper, 2004), will be required to determine the types and amounts of transcripts that change in those host cells that directly bind symbionts, compared to adjacent epithelial cells. Also, future studies will determine whether the observed changes in gene expression are either transient, and thus specific to these early events, or part of a longer-term or permanent change in response to the symbiont. Sequential waves of transcriptomic changes have been detected following induction of different immune responses in influenza-infected lungs (Pommerenke et al., 2012), a kinetic pattern that may also occur during the subsequent 3–5 hr transit of *V. fischeri* cells from the surface to the deep crypts.

In summary, the squid-vibrio system provides an ideal candidate for testing recent models of epithelial selection, which predict parameters that favor particular bacterial species and stabilize a host-bacteria mutualism (Schluter and Foster, 2012). This study has afforded a window into initial animal-host responses to a bacterial partner, and the rapid development of new sequencing technologies promises to provide robust methods for the study of single-cell transcriptomics for bacteria such as *V. fischeri*. These horizons will present the opportunity to eavesdrop into the very first conversations of an animal host with its coevolved partner.

EXPERIMENTAL PROCEDURES

Adult *E. scolopes* were collected in Oahu (Hawaii) and bred in the laboratory. All experiments conform to the relevant regulatory standards established by the University of Wisconsin-Madison.

Transcriptomic Database Using 454 Pyrosequencing

Juvenile animals were collected within 15 min of hatching and randomly segregated into various experimental conditions in HOSW, which contains ~10^6 environmental bacteria/ml but undetectable *V. fischeri*: hatchling, aposymbiotic, and symbiotic (with ~5,000 cells/ml of strain ES114 added to the HOSW). Light organs were dissected and placed into RNA*later* (Ambion) (n = 400 per condition for 454 sequencing) and frozen at −80°C until RNA extraction (RNeasy kit, QIAGEN). cDNA was generated (SMART cDNA synthesis kit, Clontech Laboratories), and its quality was checked using a 2100 Bioanalyzer (Agilent Technologies). Samples were prepared for the 454 sequencing and sequenced on a GS FLX system with Titanium chemistry (Roche Life Sciences). Sequences were processed and assembled through Newbler, annotated for BLAST results and GO by Blast2GO, and clustered in orthologous groups. Reads were quantified (RSEM package, R software), and their differential expression was estimated using Stekel's method (R_j > 3 were differentially expressed) and FatiGO software. For details and references, see Supplemental Experimental Procedures.

Expression of Candidate Genes

Squid were collected as for the 454 sequencing, with an additional "sterile" condition in filter-sterilized Instant Ocean (FSIO). qRT-PCR procedures conform to the Minimum Information for Publication of Quantitative Real-Time PCR Experiments (MIQE) guidelines (Bustin et al., 2009) for light-organ collection (20 squid per replicate), RNA preparation, cDNA preparation, qPCR amplification, expression normalization against three housekeeping genes, and data analysis.

Full-length sequence was confirmed by RACE. In situ probes were synthetized from cDNA using a T7 polymerase (Promega) and primers containing the T7-binding site at the 5′ end. Whole-mount ISHs were performed as described in Lee et al. (2009) with incubations at 60°C. For details, see Supplemental Experimental Procedures.

Immunocytochemistry and Protein Biochemistry

Polyclonal antibodies against the squid chitotriosidase and chitin synthase were generated from synthetic peptides made to unique regions in the protein (GenScript) and were determined to be highly specific by western blot when used against squid protein extracts. For immunocytochemistry (ICC), the fixation, permeabilization, blocking, and washing procedures were modified from Troll et al., 2010 (see Supplemental Experimental Procedures). For ICC experiments involving mucus staining, the procedure was identical to classical ICCs, except that squid were fixed in Bouin's solution for 3 hr and permeabilized for 2 hr, and the mucus was counterstained with 10 μg/ml Alexa 633-conjugated WGA.

The chitotriosidase was purified by affinity chromatography: squid protein extract was incubated for 1 hr at 4°C with 50 μl of prewashed chitin bound to magnetic beads (New England Biolabs). Unbound proteins were washed, and purified proteins were loaded (after beads were boiled for 10 min in 1X TCEP-loading buffer) into a NuPAGE 4%–12% Bis-Tris gel and stained with SYPRO Ruby (Life Technologies). Chitotriosidase activity was tested using a chitinase assay kit (Sigma-Aldrich) on the bead-protein complex against 50 μg of 4-methylumbelliferyl-β-D-N,N′,N″-triacetylchitotriose, which fluoresces at 535 nm after cleavage by chitotriosidase (for details, see Supplemental Experimental Procedures).

Determination of Mucus pH

WGA (Vector Laboratories), which labels host mucus, was mixed with the dual-emission pH probe SNARF-4F 5-(and 6-)-carboxylic acid (SNARF, Molecular Probes) at a 1:10 ratio for 15 min with agitation. SNARF was covalently linked to WGA by incubating EDAC at a 1:10 ratio with the protein overnight at 4°C, a reaction that was quenched by adding 1 M glycine. Free SNARF was rinsed from the protein by filtration through Amicon Ultra-4 Centrifugal Filter Units (Millipore) with mPBS. A calibration curve of SNARF, at a working concentration of 10 μM in mPBS at pH values from 5.5 to 8, was generated after excitation at 488 nm. Squid were incubated for 30 min in 10 μg/ml WGA-SNARF in FSIO and washed three times in FSIO before anesthesia. The signal intensity in 100 μm^2 squares was measured at 580 nm and 650 nm emissions.

Localization of Chitin Derivatives

The 3 hr squid were incubated with a mix of 20 μg/ml of Alexa 633 WGA, which stains GlcNAc residues and sialic acid; 20 μg/ml of fluorescein isothiocyanate (FITC)-succinylated WGA, which stains GlcNAc residues only; and 10 mM CellTracker Orange in FSIO for 30 min. Squid were washed three times in FSIO and anesthetized before mounting. To localize chitin in the light organ, squid were incubated in 1% calcofluor white, which intercalates into chitin and cellulose, in FSIO for 5 min following the manufacturer's instructions (Sigma-Aldrich). For FITC-conjugated chitin-binding protein (CBP; New England Biolabs) staining, squid were fixed and permeabilized as for the ICC protocol in mucus, and CBP was added at a dilution of 1:250 in mPBS for 3 days.

Capillary Assays for Chemoattraction

Chemotaxis toward 10 mM chitobiose was measured in 1 μl capillary tubes after growth in seawater tryptone medium (SWT) supplemented or not with 1 mM chitobiose ($(GlcNAc)_2$). Nonprimed cells showed chemotaxis toward GlcNAc (Figure S3), which indicated that they were both motile and chemotactic. To further control for any indirect effects during growth in the presence of a sugar, we measured chemotaxis toward chitobiose by *V. fischeri* cells that were pre-exposed to either 100 μM or 1 mM GlcNAc and observed no response (fewer than 4,000 colony-forming units [cfu] per capillary, data not shown). For details, see Supplemental Experimental Procedures.

Squid Colonization after Chitotriosidase Inhibition

Squid were preincubated in 12-well plates for 2 hr in 2 ml FSIO+IgG, i.e., FSIO containing either α-EsChitotriosidase antibody (20 μg/ml) to bind specific sites or rabbit IgG (20 μg/ml, GenScript) as a control (six squid per well, three wells per condition). Squid were then transferred for 3 hr into FSIO+IgG containing either 3,000 or 5,000 *V. fischeri* per ml. Squid were quickly rinsed to stop colonization, transferred into FSIO+IgG, and incubated overnight. Luminescence was scored after 18 hr in a luminometer (Turner Designs), and bacterial density was checked at the end of the experiment to ensure a similar inoculation for both conditions. Because colonization data follow a binomial distribution, statistics were calculated using the Fisher's exact test (R software, version 2.14.1). Control with 20 μg/ml of bovine serum albumin (BSA) was also performed to rule out any potential effect of the IgG (Fisher's exact test between IgG and BSA; 3,000 cfu/ml, $p = 0.71$; 5,000 cfu/ml, $p = 1.00$). Reduction of chitotriosidase activity against 4-methylumbelliferyl-β-D-N,N′,N″-triacetylchitotriose was tested in vitro as described above, with no addition, addition of 40 μg of α-EsChit antibody, or addition of rabbit IgG ($n = 3$ replicates per condition).

ACCESSION NUMBERS

Sequences were deposited in the Sequence Read Archive under the biological project PRJNA205147. The GenBank accession number of *EsChitotriosidase* is KF015222.

SUPPLEMENTAL INFORMATION

Supplemental Information includes Supplemental Experimental Procedures, three figures, and one table and can be found with this article online at http://dx.doi.org/10.1016/j.chom.2013.07.006.

ACKNOWLEDGMENTS

We thank Fabrice Vavre for helpful discussions and Dorina Ölsner for assistance. This work was supported by NIH grants AI50661 to M.J.M.-N. and RR12294 to E.G.R. and M.J.M.-N.; NSF grant IOS 0817232 to M.J.M.-N. and E.G.R.; the DFG priority program 1399, Genomics Analysis Platform RO2994, and structural funds of the DFG Clusters of Excellence EXC306, "Inflammation at Interfaces," and EXC80, "The Future Ocean," to P.R.; and Marie Curie Actions grant FP7-PEOPLE-2010-IOF/272684/SymbiOx to N.K.

Received: May 7, 2013
Revised: June 12, 2013
Accepted: June 24, 2013
Published: August 14, 2013

REFERENCES

Altura, M.A., Heath-Heckman, E.A.C., Gillette, A., Kremer, N., Krachler, A.M., Brennan, C.A., Ruby, E.G., Orth, K., and McFall-Ngai, M.J. (2013). First engagement of partners in the *Euprymna scolopes-Vibrio fischeri* symbiosis is a two-step process initiated by a few environmental symbiont cells. Environ. Microbiol. Published online June 11, 2013. http://dx.doi.org/10.1111/1462-2920.12179.

Alvarez-Ordóñez, A., Begley, M., Prieto, M., Messens, W., López, M., Bernardo, A., and Hill, C. (2011). *Salmonella* spp. survival strategies within the host gastrointestinal tract. Microbiology *157*, 3268–3281.

Badariotti, F., Thuau, R., Lelong, C., Dubos, M.-P., and Favrel, P. (2007). Characterization of an atypical family 18 chitinase from the oyster *Crassostrea gigas*: evidence for a role in early development and immunity. Dev. Comp. Immunol. *31*, 559–570.

Bassler, B.L., Gibbons, P.J., Yu, C., and Roseman, S. (1991). Chitin utilization by marine bacteria. Chemotaxis to chitin oligosaccharides by *Vibrio furnissii*. J. Biol. Chem. *266*, 24268–24275.

Benkert, P., Biasini, M., and Schwede, T. (2011). Toward the estimation of the absolute quality of individual protein structure models. Bioinformatics *27*, 343–350.

Blokesch, M., and Schoolnik, G.K. (2007). Serogroup conversion of *Vibrio cholerae* in aquatic reservoirs. PLoS Pathog. *3*, e81.

Blümer, N., Pfefferle, P.I., and Renz, H. (2007). Development of mucosal immune function in the intrauterine and early postnatal environment. Curr. Opin. Gastroenterol. *23*, 655–660.

Bry, L., Falk, P.G., Midtvedt, T., and Gordon, J.I. (1996). A model of host-microbial interactions in an open mammalian ecosystem. Science *273*, 1380–1383.

Bustin, S.A., Benes, V., Garson, J.A., Hellemans, J., Huggett, J., Kubista, M., Mueller, R., Nolan, T., Pfaffl, M.W., Shipley, G.L., et al. (2009). The MIQE guidelines: minimum information for publication of quantitative real-time PCR experiments. Clin. Chem. *55*, 611–622.

Carlson, S.A., Sharma, V.K., McCuddin, Z.P., Rasmussen, M.A., and Franklin, S.K. (2007). Involvement of a *Salmonella* genomic island 1 gene in the rumen protozoan-mediated enhancement of invasion for multiple-antibiotic-resistant *Salmonella enterica* serovar Typhimurium. Infect. Immun. *75*, 792–800.

Cho, J.H., Park, I.Y., Kim, H.S., Lee, W.T., Kim, M.S., and Kim, S.C. (2002). Cathepsin D produces antimicrobial peptide parasin I from histone H2A in the skin mucosa of fish. FASEB J. *16*, 429–431.

Chun, C.K., Scheetz, T.E., Bonaldo, Mde.F., Brown, B., Clemens, A., Crookes-Goodson, W.J., Crouch, K., DeMartini, T., Eyestone, M., Goodson, M.S., et al. (2006). An annotated cDNA library of juvenile *Euprymna scolopes* with and without colonization by the symbiont *Vibrio fischeri*. BMC Genomics *7*, 154.

Conus, S., and Simon, H.-U. (2010). Cathepsins and their involvement in immune responses. Swiss Med. Wkly. *140*, w13042.

Davidson, S.K., Koropatnick, T.A., Kossmehl, R., Sycuro, L., and McFall-Ngai, M.J. (2004). NO means 'yes' in the squid-vibrio symbiosis: nitric oxide (NO)

during the initial stages of a beneficial association. Cell. Microbiol. *6*, 1139–1151.

Dinglasan, R.R., Devenport, M., Florens, L., Johnson, J.R., McHugh, C.A., Donnelly-Doman, M., Carucci, D.J., Yates, J.R., 3rd, and Jacobs-Lorena, M. (2009). The *Anopheles gambiae* adult midgut peritrophic matrix proteome. Insect Biochem. Mol. Biol. *39*, 125–134.

Duerkop, B.A., Vaishnava, S., and Hooper, L.V. (2009). Immune responses to the microbiota at the intestinal mucosal surface. Immunity *31*, 368–376.

Eberl, G. (2012). Development and evolution of RORγt+ cells in a microbe's world. Immunol. Rev. *245*, 177–188.

Fraune, S., Augustin, R., Anton-Erxleben, F., Wittlieb, J., Gelhaus, C., Klimovich, V.B., Samoilovich, M.P., and Bosch, T.C.G. (2010). In an early branching metazoan, bacterial colonization of the embryo is controlled by maternal antimicrobial peptides. Proc. Natl. Acad. Sci. USA *107*, 18067–18072.

Fusetti, F., von Moeller, H., Houston, D., Rozeboom, H.J., Dijkstra, B.W., Boot, R.G., Aerts, J.M.F.G., and van Aalten, D.M.F. (2002). Structure of human chitotriosidase. Implications for specific inhibitor design and function of mammalian chitinase-like lectins. J. Biol. Chem. *277*, 25537–25544.

Heath-Heckman, E.A.C., and McFall-Ngai, M.J. (2011). The occurrence of chitin in the hemocytes of invertebrates. Zoology (Jena) *114*, 191–198.

Hegedus, D., Erlandson, M., Gillott, C., and Toprak, U. (2009). New insights into peritrophic matrix synthesis, architecture, and function. Annu. Rev. Entomol. *54*, 285–302.

Hirano, T., Aoki, M., Kadokura, K., Kumaki, Y., Hakamata, W., Oku, T., and Nishio, T. (2011). Heterodisaccharide 4-O-(*N*-acetyl-β-D-glucosaminyl)-D-glucosamine is an effective chemotactic attractant for *Vibrio* bacteria that produce chitin oligosaccharide deacetylase. Lett. Appl. Microbiol. *53*, 161–166.

Hooper, L.V. (2004). Laser microdissection: exploring host-bacterial encounters at the front lines. Curr Opin Microbiol *7*, 290–295.

Kimbell, J.R., Koropatnick, T.A., and McFall-Ngai, M.J. (2006). Evidence for the participation of the proteasome in symbiont-induced tissue morphogenesis. Biol. Bull. *211*, 1–6.

Krukonis, E.S., and DiRita, V.J. (2003). From motility to virulence: Sensing and responding to environmental signals in *Vibrio cholerae*. Curr. Opin. Microbiol. *6*, 186–190.

Lee, P.N., McFall-Ngai, M.J., Callaerts, P., and de Couet, H.G. (2009). Whole-mount in situ hybridization of Hawaiian bobtail squid (*Euprymna scolopes*) embryos with DIG-labeled riboprobes: II. Embryo preparation, hybridization, washes, and immunohistochemistry. Cold Spring Harb. Protoc. *2009*, pdb.prot5322.

Lee, C.G., Da Silva, C.A., Dela Cruz, C.S., Ahangari, F., Ma, B., Kang, M.-J., He, C.-H., Takyar, S., and Elias, J.A. (2011). Role of chitin and chitinase/chitinase-like proteins in inflammation, tissue remodeling, and injury. Annu. Rev. Physiol. *73*, 479–501.

Liu, X., Li-Ling, J., Hou, L., Li, Q., and Ma, F. (2009). Identification and characterization of a chitinase-coding gene from Lamprey (*Lampetra japonica*) with a role in gonadal development and innate immunity. Dev. Comp. Immunol. *33*, 257–263.

Mandel, M.J., Schaefer, A.L., Brennan, C.A., Heath-Heckman, E.A.C., Deloney-Marino, C.R., McFall-Ngai, M.J., and Ruby, E.G. (2012). Squid-derived chitin oligosaccharides are a chemotactic signal during colonization by *Vibrio fischeri*. Appl. Environ. Microbiol. *78*, 4620–4626.

McFall-Ngai, M.J., and Ruby, E.G. (1991). Symbiont recognition and subsequent morphogenesis as early events in an animal-bacterial mutualism. Science *254*, 1491–1494.

McFall-Ngai, M.J., Hadfield, M.G., Bosch, T.C.G., Carey, H.V., Domazet-Lošo, T., Douglas, A.E., Dubilier, N., Eberl, G., Fukami, T., Gilbert, S.F., et al. (2013). Animals in a bacterial world, a new imperative for the life sciences. Proc. Natl. Acad. Sci. USA *110*, 3229–3236.

Meibom, K.L., Blokesch, M., Dolganov, N.A., Wu, C.-Y., and Schoolnik, G.K. (2005). Chitin induces natural competence in *Vibrio cholerae*. Science *310*, 1824–1827.

Merrell, D.S., Hava, D.L., and Camilli, A. (2002). Identification of novel factors involved in colonization and acid tolerance of *Vibrio cholerae*. Mol. Microbiol. *43*, 1471–1491.

Miyashiro, T., Klein, W., Oehlert, D., Cao, X., Schwartzman, J., and Ruby, E.G. (2011). The *N*-acetyl-D-glucosamine repressor NagC of *Vibrio fischeri* facilitates colonization of *Euprymna scolopes*. Mol. Microbiol. *82*, 894–903.

Nyholm, S.V., Deplancke, B., Gaskins, H.R., Apicella, M.A., and McFall-Ngai, M.J. (2002). Roles of *Vibrio fischeri* and nonsymbiotic bacteria in the dynamics of mucus secretion during symbiont colonization of the *Euprymna scolopes* light organ. Appl. Environ. Microbiol. *68*, 5113–5122.

Oldroyd, G.E.D. (2013). Speak, friend, and enter: signalling systems that promote beneficial symbiotic associations in plants. Nat. Rev. Microbiol. *11*, 252–263.

Ong, D.S.T., Wang, L., Zhu, Y., Ho, B., and Ding, J.L. (2005). The response of ferritin to LPS and acute phase of *Pseudomonas* infection. J. Endotoxin Res. *11*, 267–280.

Pacheco, A.R., Curtis, M.M., Ritchie, J.M., Munera, D., Waldor, M.K., Moreira, C.G., and Sperandio, V. (2012). Fucose sensing regulates bacterial intestinal colonization. Nature *492*, 113–117.

Pommerenke, C., Wilk, E., Srivastava, B., Schulze, A., Novoselova, N., Geffers, R., and Schughart, K. (2012). Global transcriptome analysis in influenza-infected mouse lungs reveals the kinetics of innate and adaptive host immune responses. PLoS ONE *7*, e41169.

Rasmussen, M.A., Carlson, S.A., Franklin, S.K., McCuddin, Z.P., Wu, M.T., and Sharma, V.K. (2005). Exposure to rumen protozoa leads to enhancement of pathogenicity of and invasion by multiple-antibiotic-resistant *Salmonella enterica* bearing SGI1. Infect. Immun. *73*, 4668–4675.

Schluter, J., and Foster, K.R. (2012). The evolution of mutualism in gut microbiota via host epithelial selection. PLoS Biol. *10*, e1001424.

Stekel, D.J., Git, Y., and Falciani, F. (2000). The comparison of gene expression from multiple cDNA libraries. Genome Res. *10*, 2055–2061.

Troll, J.V., Bent, E.H., Pacquette, N., Wier, A.M., Goldman, W.E., Silverman, N., and McFall-Ngai, M.J. (2010). Taming the symbiont for coexistence: a host PGRP neutralizes a bacterial symbiont toxin. Environ. Microbiol. *12*, 2190–2203.

Wang, Y., Dunn, A.K., Wilneff, J., McFall-Ngai, M.J., Spiro, S., and Ruby, E.G. (2010). *Vibrio fischeri* flavohaemoglobin protects against nitric oxide during initiation of the squid-vibrio symbiosis. Mol. Microbiol. *78*, 903–915.

Wier, A.M., Nyholm, S.V., Mandel, M.J., Massengo-Tiassé, R.P., Schaefer, A.L., Koroleva, I., Splinter-Bondurant, S., Brown, B., Manzella, L., Snir, E., et al. (2010). Transcriptional patterns in both host and bacterium underlie a daily rhythm of anatomical and metabolic change in a beneficial symbiosis. Proc. Natl. Acad. Sci. USA *107*, 2259–2264.

Xu, N., and Zhang, S. (2012). Identification, expression and bioactivity of a chitotriosidase-like homolog in amphioxus: dependence of enzymatic and antifungal activities on the chitin-binding domain. Mol. Immunol. *51*, 57–65.

Yip, E.S., Geszvain, K., DeLoney-Marino, C.R., and Visick, K.L. (2006). The symbiosis regulator rscS controls the *syp* gene locus, biofilm formation and symbiotic aggregation by *Vibrio fischeri*. Mol. Microbiol. *62*, 1586–1600.